RESEARCH ARTICLE

CD70-Targeted Allogeneic CAR T-Cell Therapy for Advanced Clear Cell Renal Cell Carcinoma

Sumanta K. Pal[1], Ben Tran[2], John B.A.G. Haanen[3,4,5], Michael E. Hurwitz[6], Adrian Sacher[7,8], Nizar M. Tannir[9], Lihua E. Budde[1], Simon J. Harrison[2], Sebastian Klobuch[3], Sagar S. Patel[10], Luis Meza[1], Mary-Lee Dequeant[11], Anna Ma[11], Qiuling Ally He[11], Leah M. Williams[11], Alissa Keegan[11], Ellen B. Gurary[12], Henia Dar[11], Sushant Karnik[11], Changan Guo[12], Heidi Heath[11], Rachel R. Yuen[11], Phuong K. Morrow[12], Neeraj Agarwal[13], and Samer A. Srour[9]

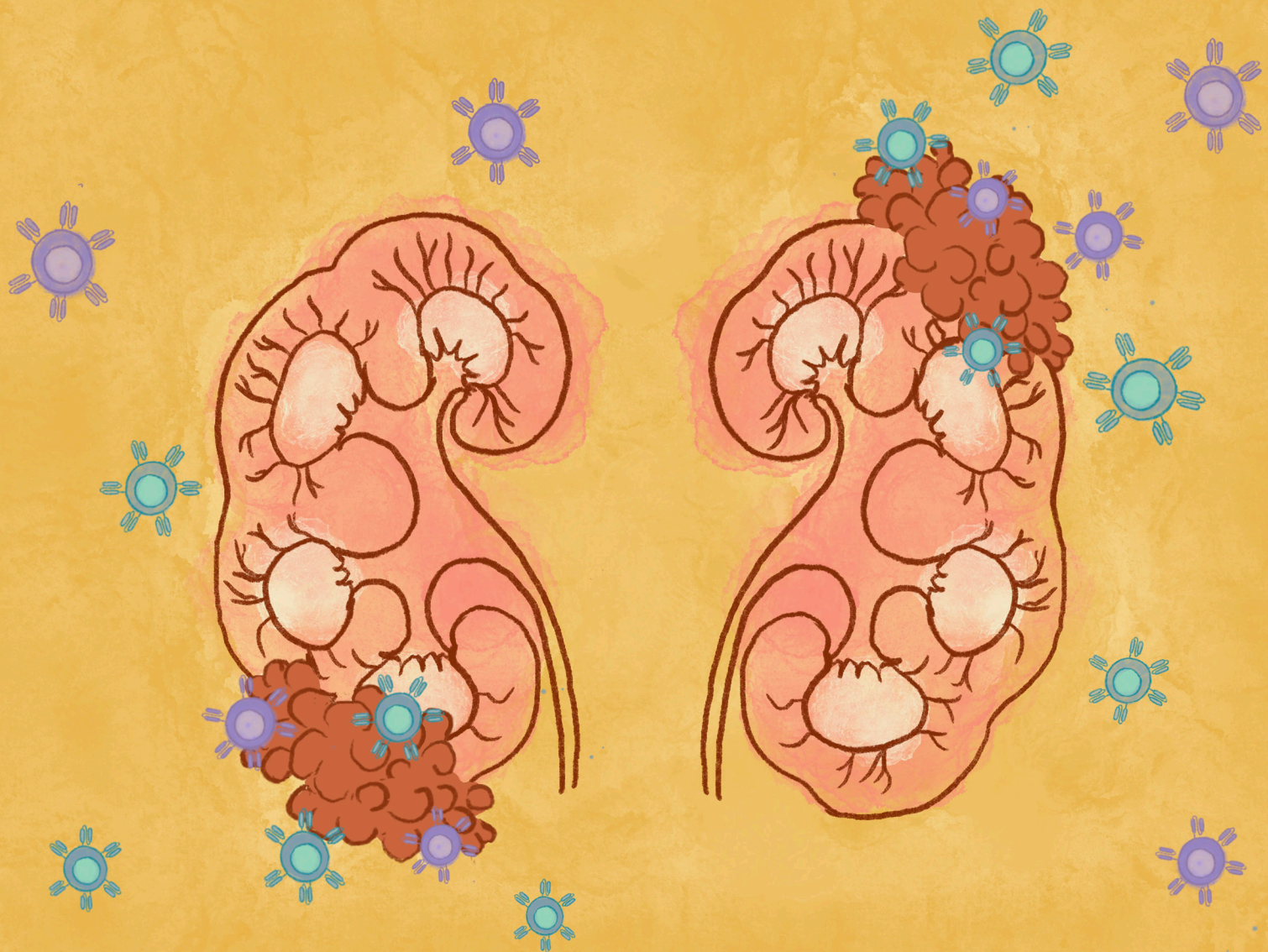

ABSTRACT Therapeutic approaches for clear cell renal cell carcinoma (ccRCC) remain limited; however, chimeric antigen receptor (CAR) T-cell therapies may offer novel treatment options. CTX130, an allogeneic CD70-targeting CAR T-cell product, was developed for the treatment of advanced or refractory ccRCC. We report that CTX130 showed favorable preclinical proliferation and cytotoxicity profiles and completely regressed RCC xenograft tumors. We also report results from 16 patients with relapsed/refractory ccRCC who received CTX130 in a phase I, multicenter, first-in-human clinical trial. No patients encountered dose-limiting toxicity, and disease control was achieved in 81.3% of patients. One patient remains in a durable complete response at 3 years. Finally, we report on a next-generation CAR T construct, CTX131, in which synergistic potency edits to CTX130 confer improved expansion and efficacy in preclinical studies. These data represent a proof of concept for the treatment of ccRCC and other $CD70^+$ malignancies with $CD70^-$ targeted allogeneic CAR T cells.

SIGNIFICANCE: Although the role of CAR T cells is well established in hematologic malignancies, the clinical experience in solid tumors has been disappointing. This clinical trial demonstrates the first complete response in a patient with RCC, reinforcing the potential benefit of CAR T cells in the treatment of solid tumors.

See corresponding author Sumanta K. Pal discuss this research article, published simultaneously at the AACR Annual Meeting 2024: https://vimeo.com/932606570/887520f9cb

INTRODUCTION

Renal cell carcinoma (RCC) accounts for approximately 3% of all cancers, with 82,000 new cases and 15,000 deaths estimated in the United States in 2023 (1, 2). Clear cell RCC (ccRCC) is the most common RCC subtype (3). Although localized disease can often be cured with partial or radical nephrectomy, approximately 30% of patients will develop metastases that require systemic therapy (3).

The success of immunotherapy in ccRCC dates back over three decades, with durable remission obtained with cytokine therapies such as interleukin-2 (IL2; refs. 4–6). The standard first-line approach to the management of patients with metastatic ccRCC includes dual immune-checkpoint inhibitor (ICI) therapy or therapy with an ICI combined with a vascular endothelial growth factor (VEGF)-directed therapy (7). These approaches result in response rates ranging from 42% to 71% (8–11). However, only a minority of patients achieve complete responses (CR); the majority will ultimately progress beyond first-line treatment and will require subsequent therapies (8–11). For patients who do not respond to prior ICI treatment, salvage treatment with VEGF-directed therapies yields median progression-free survival (PFS) in the range of 5 to 8 months, with average overall response rates (ORR) between 28% and 43% (12–14). Notably, current systemic therapies for metastatic ccRCC are applied in a continuous fashion, thereby prolonging the duration and exposure to chronic toxicities.

Cluster of differentiation (CD) 70, a member of the tumor necrosis factor superfamily, is a costimulatory molecule that is transiently expressed on specific immune cells including dendritic cells, activated lymphocytes, antigen-presenting cells in the gut lamina propria, and T cells in the tonsils, skin, and intestines (1, 15–18). Current evidence suggests that signaling through CD70 and its receptor (CD27) may support tumoral growth by limiting inflammatory T-cell expansion, driving the proliferation of immune-suppressive T-regulatory cells, and enabling immune evasion (16, 19–21). Elevated and stable expression of CD70 has been detected in multiple tumor types, including several lymphoid malignancies, pancreatic cancer, glioblastoma, and ccRCC, with minimal expression in normal tissues (1, 17, 22, 23). In a retrospective immunohistochemistry (IHC)-based study, CD70 expression was detected in 58% of lymphoma samples, 43% of solid tumor samples, and 80% of ccRCC samples (16). Notably, CD70 is considered by some to be a biomarker for ccRCC (1). CD70 expression is regulated by hypoxia-inducible factor (HIF); mutations in the von Hippel–Lindau gene in the majority of ccRCC stabilize HIF, allowing for the activation of CD70 and its downstream targets (24). Aberrant expression of CD70 in RCC appears to drive terminal

[1]Department of Medical Oncology, City of Hope Comprehensive Cancer Center, Duarte, California. [2]Department of Medical Oncology, Peter MacCallum Cancer Centre, Melbourne, Australia. [3]Netherlands Cancer Institute, Amsterdam, the Netherlands. [4]Leiden University Medical Center, Leiden, the Netherlands. [5]Centre Hospitalier Universitaire Vaudois, Lausanne, Switzerland. [6]Yale School of Medicine, New Haven, Connecticut. [7]Princess Margaret Cancer Centre, University Health Network, Toronto, Canada. [8]Departments of Medicine and Immunology, University of Toronto, Toronto, Canada. [9]University of Texas MD Anderson Cancer Center, Houston, Texas. [10]Division of Hematology and Hematologic Malignancies, Huntsman Cancer Institute, University of Utah, Salt Lake City, Utah. [11]CRISPR Therapeutics, Boston, Massachusetts. [12]Formerly employed by CRISPR Therapeutics, Boston, Massachusetts. [13]Division of Medical Oncology, Huntsman Cancer Institute, University of Utah, Salt Lake City, Utah.

ClinicalTrials.gov number: NCT04438083.

Corresponding Author: Sumanta K. Pal, City of Hope Comprehensive Cancer Center, 1500 East Duarte Road, Duarte, CA 91010. E-mail: spal@coh.org

Cancer Discov 2024;14:1176–89

doi: 10.1158/2159-8290.CD-24-0102

T-cell differentiation and lymphocyte apoptosis (17, 20, 23, 25). Therefore, anti-CD70 targeting is being explored as a possible therapeutic option for CD70-expressing tumor types.

Several early-phase clinical trials have explored the role of CD70-targeted agents, including monoclonal antibodies and antibody–drug conjugates, in RCC. These agents have demonstrated limited success in ccRCC, with overall acceptable safety profiles and disease control rates (DCR) ranging from 22% to 78% but no instances of CR (21, 22, 26–28).

CTX130 is an investigational, first-in-class, CD70-targeted allogeneic chimeric antigen receptor (CAR) T-cell therapy. CTX130 is modified with CRISPR-Cas9 gene editing to (i) insert an anti-CD70 CAR expression cassette into the T-cell receptor alpha constant (TRAC) locus, (ii) disrupt β2-microglobulin (β2M) to eliminate major histocompatibility complex (MHC) class I surface expression (29), and (iii) disrupt CD70 expression to mitigate fratricide and enhance performance. The precise insertion of the anti-CD70 CAR expression cassette is enabled by homology-directed repair.

We describe preclinical *in vitro* and *in vivo* results demonstrating the efficacy and antitumor activity of CTX130 and results from the phase I COBALT-RCC clinical trial (ClinicalTrials.gov number NCT04438083), in which patients with ccRCC were infused with CTX130 at varying dose levels. We also show that a modified version of CTX130 (CTX131) incorporating knockout (KO) of Regnase-1 and transforming growth factor β receptor 2 (TGFβR2) demonstrates improved expansion and potency relative to CTX130 in preclinical models and therefore has potential as an improved treatment option for patients with ccRCC.

RESULTS

CTX130: *In Vitro* Studies

To assess the benefit of CD70 disruption to the CTX130 profile, assays were designed to compare CTX130 activity with that of an isogenic anti-CD70 CAR T retaining the intact CD70 locus (CD70$^+$ anti-CD70 CAR T cells). Cell proliferation assays revealed that CTX130 displayed increased (9-fold at day 12 after electroporation) cell expansion relative to CD70$^+$ anti-CD70 CAR T cells (Fig. 1A). Flow cytometry performed on CTX130 cells at day 7 after electroporation revealed that most cells were T-cell receptor (TCR)-negative (>98%) and CD70-negative (>98%). Flow-cytometric analysis also revealed that >97% of CD70$^+$ anti-CD70 CAR T cells were TCR-negative and >97% were CD70-negative. Approximately 13% of unedited control T cells exhibited CD70 expression, suggesting fratricide during the manufacturing of CD70$^+$ anti-CD70 CAR T cells.

CTX130 and CD70$^+$ anti-CD70 CAR T cells were also assessed for cytotoxic activity after an increasing number of challenges with CD70$^+$ A498 RCC cells. In these assays, multiple rounds of tumor cells were added to the CAR T cells to assess repetitive tumor-killing potential and CAR T-cell exhaustion. CTX130 exhibited sustained cell-killing activity for ≥13 challenges, whereas CD70$^+$ anti-CD70 CAR T cells lost their cell-killing activity after 9 challenges (Fig. 1B).

In vitro cytotoxicity studies were also conducted to demonstrate the specificity of CTX130 for CD70$^+$ cells (Fig. 1C). CTX130 cells were cocultured with CD70^{high} (A498), CD70^{low} (ACHN), and CD70$^-$ (MCF7) cells, and cytotoxicity was assessed using a luminescence-based cell viability assay. CTX130 was cytotoxic toward both CD70^{low} and CD70^{high} cells. However, the cytotoxicity of CTX130 and unedited T cells were similar upon coculture with a CD70$^-$ cell line.

CTX130: *In Vivo* Efficacy Studies

To understand the impact of CD70 disruption in CTX130 on antitumor activity *in vivo*, a study was conducted comparing the A498 RCC xenograft tumor response to CTX130 (n = 5) with the response to CD70$^+$ anti-CD70 CAR T cells (n = 4; both dosed at approximately 8 million CAR$^+$ T cells). Administration of CTX130 resulted in complete tumor regression, whereas administration of CD70$^+$ anti-CD70 CAR T cells resulted in no significant antitumor activity (Fig. 1D).

To evaluate the potential benefit of disruption of the checkpoint gene programmed cell death 1 (PD-1), which has been reported to improve potency in other CAR T-cell products (30–32), we compared the ability of CTX130 (TRAC$^-$/β2M$^-$/CD70$^-$) with or without PD-1 KO (PD1$^-$) to eradicate tumors in an A498 subcutaneous xenograft rechallenge model. Within 2 weeks, the CAR T cells cleared the initial 50 mm^3 tumor in all mice. Fresh tumor cells were then implanted subcutaneously on the opposite flank 24 days after initial dosing. Following the rechallenge, CTX130 completely inhibited tumor growth in all 5 mice. Meanwhile, PD-1 KO reduced CAR T potency, as evidenced by the tumor growth observed in 4 of 5 mice treated with CTX130 with PD-1 KO (TRAC$^-$/β2M$^-$/CD70$^-$/PD1$^-$; Fig. 1E; ref. 33).

To investigate the ability of disruption of the TCR in CTX130 to reduce the risk of graft versus host disease (GvHD), immunocompromised mice were irradiated and then administered a single dose of either unedited T cells or CTX130 (low dose, 20 million cells/mouse; high dose, 40 million cells/mouse). Mice were then monitored for symptoms of GvHD through-out a 12-week period. Mice that received unedited T cells developed fatal GvHD within 21 days of dosing, whereas all mice in the CTX130 dose groups survived to the 12-week endpoint (Fig. 1F).

Figure 1. Preclinical efficacy and antitumor activity of CTX130. **A,** Proliferation of CTX130 versus CD70$^+$ CAR T cells. **B,** CTX130 and CD70$^+$ anti-CD70 CAR T-cell cytotoxicity as a percentage of cell lysis after repeated challenges with CD70$^+$ A498 cells. Data points represent a single measurement. **C,** CTX130 cytotoxicity toward CD70^{high} (A498), CD70^{low} (ACHN), and CD70$^-$ (MCF7) cell lines. Results from cells treated with CTX130 are shown with solid circles, and results from cells treated with unedited T cells are shown with open squares. The graph shows the mean ± SD from 3 technical replicates with increasing ratios of CTX130 or unedited T cells to tumor cells (0.125:1 to 4:1). **D,** Antitumor activity of CAR T cells in an RCC xenograft model. Mice were either left untreated (n = 5) or injected with CTX130 (n = 5) or CD70$^+$ anti-CD70 CAR T cells (n = 4). Each point represents the mean tumor volume ± SEM. **E,** Disruption of the PD-1 checkpoint gene is detrimental to CTX130 CAR T-cell function in a xenograft rechallenge model. Following the first injection of tumor cells, mice (n = 5 per group) were left untreated (open circles) or treated with CTX130 (open squares) or PD1$^-$ CTX130 CAR T cells (open triangles). At the day 25 rechallenge, fresh tumor cells were injected into the left flank of treated mice (CTX130-treated and PD1$^-$ CTX130-treated animals represented by solid circles and solid triangles, respectively) and a new control group (open lozenges). Each point represents the mean tumor volume ± SEM. **F,** Mortality due to GvHD in mice (n = 30 per group) treated with unedited T cells or low (20 million cells/mouse) or high (40 million cells/mouse) doses of CTX130. CAR, chimeric antigen receptor; CD, cluster of differentiation; EP, electroporation; GvHD, graft versus host disease; KO, knockout; PD-1, programmed cell death 1; RCC, renal cell carcinoma.

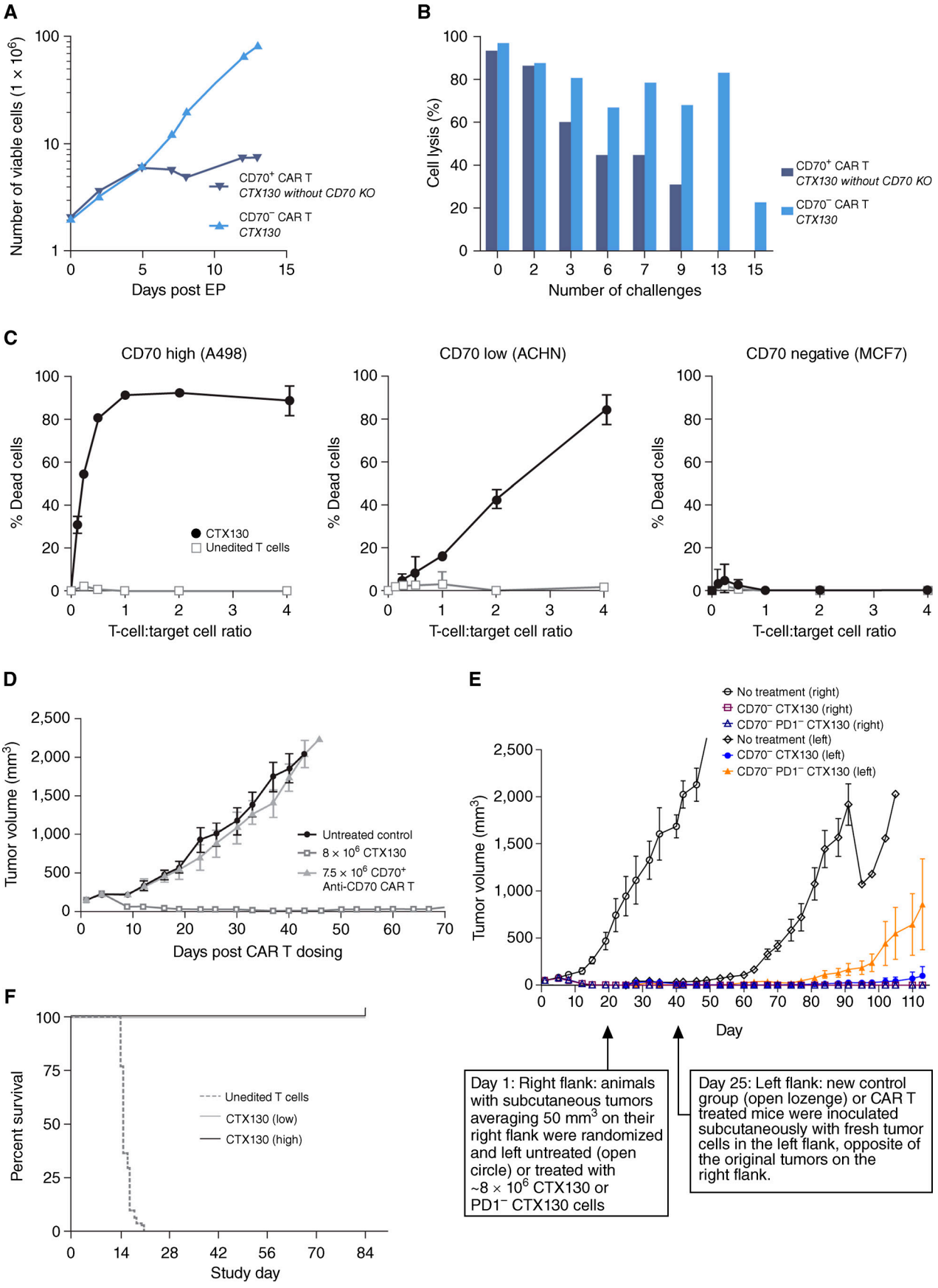
A
Number of viable cells (1 × 10^6)
Days post EP
CD70+ CAR T
CTX130 without CD70 KO
CD70− CAR T
CTX130
B
Cell lysis (%)
Number of challenges
CD70+ CAR T
CTX130 without CD70 KO
CD70− CAR T
CTX130
C
CD70 high (A498)
CD70 low (ACHN)
CD70 negative (MCF7)
% Dead cells
T-cell:target cell ratio
CTX130
Unedited T cells
D
Tumor volume (mm3)
Days post CAR T dosing
Untreated control
8 × 10^6 CTX130
7.5 × 10^6 CD70+
Anti-CD70 CAR T
E
No treatment (right)
CD70− CTX130 (right)
CD70− PD1− CTX130 (right)
No treatment (left)
CD70− CTX130 (left)
CD70− PD1− CTX130 (left)
Tumor volume (mm3)
Day
Day 1: Right flank: animals with subcutaneous tumors averaging 50 mm3 on their right flank were randomized and left untreated (open circle) or treated with ~8 × 10^6 CTX130 or PD1− CTX130 cells
Day 25: Left flank: new control group (open lozenge) or CAR T treated mice were inoculated subcutaneously with fresh tumor cells in the left flank, opposite of the original tumors on the right flank.
F
Percent survival
Study day
Unedited T cells
CTX130 (low)
CTX130 (high)

Table 1. Patient demographics and disease characteristics in safety analysis set at baseline.

	DL1 (3×10^7 cells)	DL2 (1×10^8 cells)	DL3 (3×10^8 cells)	DL4 (9×10^8 cells)	Total
	N = 3	*N* = 3	*N* = 6	*N* = 4	*N* = 16
Median age, y (range)	59.0 (58–64)	60.0 (54–65)	61.0 (53–73)	70.0 (66–77)	63.0 (53–77)
Sex at birth, male, *n* (%)	3 (100.0)	3 (100.0)	6 (100.0)	2 (50.0)	14 (87.5)
Metastatic disease, *n* (%)	3 (100.0)	3 (100.0)	6 (100.0)	4 (100.0)	16 (100.0)
Prior anticancer therapies, *n* (%)					
Systemic therapy	3 (100.0)	3 (100.0)	6 (100.0)	4 (100.0)	16 (100.0)
Radiotherapy	1 (33.3)	2 (66.7)	4 (66.7)	4 (100.0)	11 (68.8)
Surgery	3 (100.0)	3 (100.0)	5 (83.3)	4 (100.0)	15 (93.8)
Median prior lines of systemic therapy, *n* (range)	2 (1–3)	3 (2–4)	3 (1–5)	3 (2–6)	3 (1–6)
Median time from diagnosis, y (range)	3.4 (2.5–6.3)	2.7 (0.7–3.3)	5.1 (2.5–6.3)	10.5 (5.1–24.0)	4.9 (0.7–24.0)
IMDC category at screening, *n* (%)					
Favorable	0 (0.0)	0 (0.0)	0 (0.0)	0 (0.0)	0 (0.0)
Intermediate	3 (100.0)	3 (100.0)	3 (50.0)	1 (25.0)	10 (62.5)
Poor	0 (0.0)	0 (0.0)	3 (50.0)	3 (75.0)	6 (37.5)
eGFR <60 mL/min/1.73 m^2, *n* (%)	2 (66.7)	1 (33.0)	1 (16.7)	2 (50.0)	6 (37.5)

Abbreviations: DL, dose level; eGFR, estimated glomerular filtration rate; IMDC, International Metastatic Renal Cell Carcinoma Database Consortium.

COBALT-RCC Trial: Patient Demographics

COBALT-RCC (NCT04438083) is an open-label, multicenter, phase I study evaluating the safety, efficacy, and pharmacokinetics of CTX130 in patients with relapsed/refractory unresectable or metastatic ccRCC. As of October 9, 2023, 16 patients (median age 63; range, 53–77 years) had undergone lymphodepletion [daily, intravenous (i.v.) delivery of 30 mg/m^2 fludarabine and 500 mg/m^2 for 3 days] and had received CTX130 at dose levels (DLs) ranging from 3×10^7 to 9×10^8 CAR T cells. Three patients were treated with DL1 (3×10^7 CAR T cells), including 2 patients who received a single infusion and 1 patient who received 2 infusions of CTX130. All 3 patients treated at DL2 (1×10^8 CAR T cells) received a single infusion of CTX130. At DL3 (3×10^8 CAR T cells), 4 patients received a single infusion, and 2 patients received 2 infusions. At DL4 (9×10^8 CAR T cells), 1 patient received a single infusion, and 3 patients received 2 infusions.

Table 1 summarizes baseline patient demographics and disease characteristics. Patients were predominantly (88%) male. All patients had advanced metastatic disease at enrollment and were heavily pretreated, with a median of 3 (range, 1–6) prior lines of systemic treatment (including prior exposure to both an ICI and a VEGF inhibitor). Four patients received prior anticytotoxic T-lymphocyte-associated protein 4 (CTLA4) therapy (all ipilimumab). In terms of prior tyrosine kinase inhibitors, 12 patients received cabozantinib, 7 received sunitinib, 3 received pazopanib, 3 received lenvatinib, and 3 received axitinib. Data on the presence or absence of sarcomatoid or rhabdoid histologic features were collected, but not uniformly, and were available for 11 of 16 subjects. Of these 11 subjects, 3 had sarcomatoid features only, 1 had both sarcomatoid and rhabdoid features, and 7 had neither. All patients had intermediate or poor risk disease, as classified per the International Metastatic Renal Cell Carcinoma Database Consortium (34).

COBALT-RCC Trial: Safety Results

All 16 patients who received ≥1 CTX130 infusion were included in the safety analysis set. Eight (50%) patients experienced grade 1 or 2 cytokine release syndrome (CRS); there were no grade ≥3 CRS events (Table 2), as assessed by the American Society for Transplantation and Cellular Therapy criteria (35). Four (25%) patients experienced serious adverse events (SAE) related to CTX130; all were CRS events. The median time to CRS onset was 1 day, with a median duration of 2 days. No patients experienced immune effector cell–associated neurotoxicity syndrome (ICANS) or GvHD. Three (19%) patients had SAEs of infections, all unrelated to CTX130, including a grade 5 pneumonia that occurred after disease progression and the start of subsequent anticancer therapy. There was one (6%) instance of a grade 1 infusion-related reaction. There were no instances of tumor lysis syndrome, hemophagocytic lymphohistiocytosis, or secondary malignancies. An acceptable safety profile was observed across all DLs, including no dose-limiting toxicities (DLT). Supplementary Table S1 summarizes treatment-emergent adverse events (AE) related to CTX130.

COBALT-RCC Trial: Efficacy Results

Of the 16 patients who received ≥1 CTX130 infusion and were included in the full efficacy analysis set, 13 (81%) achieved disease control [CR, partial response (PR), or stable disease (SD)], including 12 (75%) patients with SD and 1 (6%) patient with a CR (Fig. 2A; Table 3). During periods of disease stabilization, patients did not receive any additional anticancer therapies. Notably, the patient exhibiting a CR remains

Table 2. Report of CRS, ICANS, GvHD, and infections in safety analysis set by dose level.

	DL1 (3×10^7)		DL2 (1×10^8)		DL3 (3×10^8)		DL4 (9×10^8)		Total	
CAR T-cell dose	$N = 3$		$N = 3$		$N = 6$		$N = 4$		$N = 16$	
	Gr 1/2	Gr ≥3	Gr 1/2	Gr ≥3	Gr 1/2	Gr ≥3	Gr 1/2	Gr ≥3	Gr 1/2	Gr ≥3
CRS, *n* (%)	–	–	–	–	4 (66.7)	–	4 (100.0)	–	8 (50.0)	–
ICANS, *n* (%)	–	–	–	–	–	–	–	–	–	–
GvHD, *n* (%)	–	–	–	–	–	–	–	–	–	–
Infections[a], *n* (%)	–	–	–	1 (33.3)	1 (16.7)	2 (33.3)	2 (50.0)	–	3 (18.8)	3 (18.8)

[a]Includes COVID-19, pneumonia, enterocolitis, urinary tract infections, upper respiratory tract infections, sinusitis, mucosal infection, folliculitis, and device-related infection.

Abbreviations: CAR, chimeric antigen receptor; COVID-19, coronavirus disease 2019; CRS, cytokine release syndrome; DL, dose level; Gr, grade; GvHD, graft versus host disease; ICANS, immune effector cell–associated neurotoxicity syndrome.

disease-free at 3 years. The median PFS was 2.9 months (95% CI, 1.7–6.0) and median overall survival (OS) was 20.5 months (95% CI, 14.3–NA).

COBALT-RCC Trial: Pharmacokinetic and CD70 Expression Results

Pharmacokinetic analysis was performed on whole blood samples utilizing a digital droplet polymerase chain reaction (ddPCR) assay specific to the CAR construct. This method allows for the characterization of CTX130 CAR T-cell expansion in each patient as copies of CTX130 per microgram of total DNA (copies/μg). CTX130 was readily detected 20 minutes after infusion. CAR T cells were then redistributed and declined to a nadir in most patients around day 2 to day 3 after infusion. This was followed by rapid expansion with peak concentration around day 7 to day 15. CTX130 cells then subsequently declined and were no longer detected by day 28 (Fig. 2B). Although the kinetics of expansion were similar across patients, the levels of expansion showed large variability, similar to that observed with autologous CAR T cells in the ZUMA-1 (36) and TRANSCEND NHL-001 (37) clinical trials. Overall, analysis of observed CTX130 peak expansion (as measured from day 5 to day 28) showed that the range of CTX130 expansion in each DL generally increased with dose (Fig. 2C).

IHC analysis was conducted to evaluate CD70 levels in pre-and posttreatment tumor biopsy samples (Fig. 2D). Pre-CTX130 treatment biopsy samples in this relapsed/refractory setting showed high CD70 tumoral expression, with a median and mean tumor CD70 positivity of 100% and 75.7%, respectively (n = 13; range, 0–100). Paired on-treatment biopsy samples were available from 9 patients collected on day 7 and 10 patients collected on day 42. Tumoral heterogeneity, but no CD70 antigen loss, was observed in the samples tested (Fig. 2E; Supplementary Fig. S1).

CTX131: Preclinical Efficacy Studies

CTX130 has also been investigated in patients with T-cell lymphoma (TCL) in the COBALT-LYM trial (38). Efficacy results in patients with TCL (including 20% CR and 73% DCR) across the same dose range were superior to those seen in patients with ccRCC in the COBALT-RCC trial, indicating inherent issues with CAR T-cell effectiveness in solid versus hematologic cancers. Thus, modification of CTX130 was explored to obtain an improved CAR T-cell product.

An *in vivo* murine T-cell screen exploring gene edit combinations that boost potency against solid tumors identified Regnase-1 combinations as among the most highly enriched hits (39). Additional empirical evaluation of edit combinations was performed *in vivo*, thereby identifying the combination of Regnase-1 and TGFβR2 disruption (40). Regnase-1 destabilizes target messenger RNAs (mRNA) through recognition of a specific stem–loop structure in the 3′ untranslated region. Regnase-1 targets include cytokine genes (e.g., *Il6*, *Il2*, and *Il12b*) and genes involved in T-cell activation (e.g., *Tnfr2*, *Ox40*, and *c-Rel*; refs. 41–43), and deletion of Regnase-1 results in cells that are long-lived and display improved persistence and effector function in tumors (44). Thus, disruption of Regnase-1 allows for the translation of cytokines and costimulatory molecules that can enhance CAR T cell expansion and reduce T-cell clearance (45). Transforming growth factor β (TGFβ) signaling reduces T-cell proliferation and activation, suppresses $CD8^+$ T-cell cytotoxic function, and can induce CAR T-cell exhaustion (46, 47). A previous study showed that TGFβ signaling can repress expression of a cytotoxic gene program (including *GzmA*, *GzmB*, *FasL*, and *IFNγ*) in T lymphocytes and that blocking this signaling can restore cytotoxic gene-expression and promote antigen-specific tumor clearance in mice (48). Therefore, disruption of TGFβR2 reduces the immunosuppressive effects of the tumor microenvironment, potentially increasing CAR T-cell activity and potency (49).

During CAR T-cell activation, $CD70^+$ RCC A498 cells were cocultured with CTX130, CTX130 + Regnase-1 KO, CTX130 + TGFβR2 KO, or CTX131, and cytokine secretion was measured in the supernatant between 0 and 48 hours (Supplementary Fig. S2). Interestingly, CTX131 showed a higher level of secretion of canonical cytokines associated with T-cell activation and cytotoxicity, including IFNγ, IL2, TNFα, CD25/IL-2Rα, IL5, and granzyme B, compared with CTX130, CTX130 + Regnase-1 KO, and CTX130 + TGFβR2 KO. These data are consistent with the increased potency of CTX131 versus CTX130 or CTX130 with single gene (Regnase-1 or TGFβR2) disruption.

The ability of CTX131 to regress established tumors and generate systemic antitumor activity was assessed using a

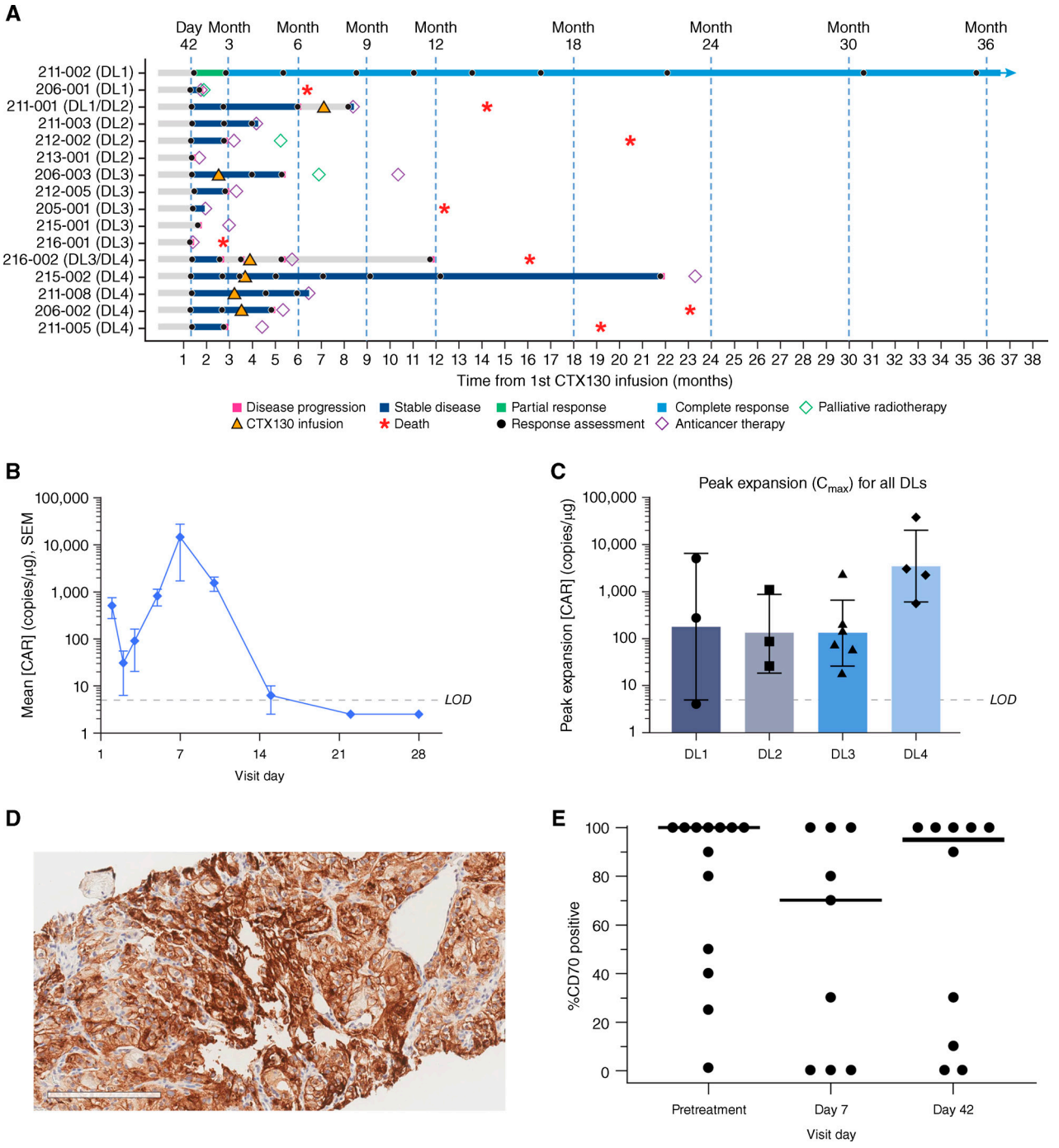

Figure 2. Clinical efficacy and pharmacokinetics of CTX130 and CD70 expression in a phase I clinical trial. **A,** Responses in COBALT-RCC participants stratified by DL received. **B,** Mean ± SEM peripheral blood concentrations of CTX130 over 28 days after first infusion at DL4 ($n = 4$). Values below the LOD were imputed as half the LOD value. **C,** Peak expansion of CTX130 in peripheral blood following the first infusion at each DL tested in the COBALT-RCC trial. Each bar represents the geometric mean ± geometric SD with each point representing the peak expansion of 1 patient ($n = 16$). **D,** Representative 20× image of CD70 IHC staining in the tumor. Scale bar, 200 µm. **E,** CD70 positivity in tumor cells before treatment ($n = 13$), day 7 after infusion ($n = 9$), and day 42 after infusion ($n = 10$). Each point represents a tumor biopsy sample from 1 patient, and bars represent median values. CAR, chimeric antigen receptor; C_{max}, peak expansion concentration; DL, dose level; IHC, immunohistochemistry; LOD, limit of detection.

xenograft rechallenge study. Treatment of mice bearing subcutaneous NCI-H1975 lung tumor xenografts with a single i.v. dose of CTX130, CTX130 + Regnase-1 KO, CTX130 + TGFβR2 KO, or CTX131 (CTX130 + Regnase-1 KO + TGFβR2 KO) generated complete tumor regression in all mice. However, only mice treated with CTX131 were able to durably clear additional rechallenges with ACHN and Caki-1 RCC tumor cells (Fig. 3A).

Table 3. Summary of response rate in the full analysis set by dose level.

CAR T-cell dose	DL1 (3×10^7) $N = 3$	DL2 (1×10^8) $N = 3$	DL3 (3×10^8) $N = 6$	DL4 (9×10^8) $N = 4$	Total $N = 16$
ORR (CR + PR), *n* (%)	1 (33.3)	0 (0.0)	0 (0.0)	0 (0.0)	1 (6.3)
CR, *n* (%)	1 (33.3)	0 (0.0)	0 (0.0)	0 (0.0)	1 (6.3)
DCR (CR + PR + SD), *n* (%)	3 (100.0)	2 (66.7)	4 (66.7)	4 (100.0)	13 (81.3)
SD, *n* (%)	2 (66.7)	2 (66.7)	4 (66.7)	4 (100.0)	12 (75.0)

Abbreviations: CAR, chimeric antigen receptor; CR, complete response; DCR, disease control rate; DL, dose level; ORR, overall response rate; PR, partial response; SD, stable disease.

Flow-cytometric analyses were performed on day 44 of the xenograft rechallenge study to assess the expansion of CAR T cells in the blood. These experiments revealed that CTX130 cells with a single KO of either Regnase-1 or TGFβR2 were present at higher levels than unmodified CTX130 cells. However, CTX131 cells were present in mouse whole blood at higher levels than unmodified CTX130 or either of the single KOs (Fig. 3B).

DISCUSSION

In the COBALT-RCC trial, which included heavily pretreated patients with ccRCC, we observed an excellent safety profile (including no grade ≥3 CRS events). The COBALT-RCC trial also demonstrated an encouraging, clinically meaningful benefit, as evidenced by a DCR of 81%. Furthermore, this trial provided evidence of the first durable CR, now persistent beyond 3 years, to a CRISPR-edited allogeneic CD70-targeting CAR T cell in solid tumors. This CR may be attributable to high tumor CD70 levels and low tumor burden.

The efficacy and safety of CTX130 have already been investigated in hematologic cancers in the COBALT-LYM trial. COBALT-LYM revealed an acceptable safety profile of CTX130 across all DLs in patients with TCL. Despite promising data, the efficacy of CTX130 in ccRCC falls short of its performance in TCL (30% CR and 70% ORR at DL ≥3; $n = 10$; ref. 38).

Given these data, it was proposed that the potency and resulting clinical activity of CTX130 could be enhanced with additional edits beyond disruption of TCR, β2M, and CD70 expression. Therefore, we have developed CTX131, a novel construct that bears the same edits as CTX130 as well as Regnase-1 disruption (to improve functional CAR T-cell persistence) and TGFβR2 disruption (to reduce the immunosuppressive effect of TGFβ in the tumor microenvironment; refs. 45, 49).

Although the role of CAR T-cell therapies is well established in hematologic malignancies, the overall clinical experience in solid tumors has been disappointing. The failure of CAR T-cell therapy in solid tumors is attributed to several mechanisms, including tumor antigen heterogeneity, the suppressive tumor microenvironment, toxicities, and in some settings, the potency of the CAR construct itself (50). Except for a few studies, the majority of early-phase CAR T-cell clinical trials in solid tumors have been challenged and stopped early either due to excessive toxicities and/or for lack of activity. Encouraging results were reported with a few autologous CAR T-cell studies targeting tumors expressing claudin 18.2 (51), interleukin-13 receptor alpha 2 (52), and disialoganglioside 2 (53). However, several other studies have been hampered by challenges including SAEs, some of which have been attributed to on-target, off-tumor toxicities (50). In a recent study assessing autologous prostate cancer–specific membrane antigen-directed CAR T cell therapy in patients with metastatic castration-resistant prostate cancer (mCRPC), no responses were observed, and 1 patient developed grade 4 CRS with hypoxic respiratory failure and capillary leak syndrome, leading to death within 30 days of treatment (54). A second study in patients with mCRPC targeting prostate cancer stem cell antigen (PSCA) was amended early due to several cases of grade 3 cystitis, possibly owing to PSCA expression on the urothelium (55). In RCC, there is limited experience with CAR T-cell therapy. One previous study assessed autologous carbonic anhydrase IX-directed CAR T cells in 12 patients with RCC. No responses were observed, and significant hepatotoxicity was noted at low DLs (56). In our study, although CD70 is transiently expressed on B cells, natural killer cells, and T cells, we observed no significant hematologic or nonhematological toxicities attributable to targeting normal tissues expressing the CD70 antigen. Furthermore, we observed encouraging antitumor activity.

Distinguishing our approach from that of several of the studies discussed above, we also employed a novel off-the-shelf CD70 CAR T-cell product derived from allogeneic healthy donor T cells. There remain several barriers to the broader applicability of autologous CAR T cells, including its labor-intensive process, cost, and more importantly the manufacturing time constraints, which would limit its use to patients with less aggressive disease. In contrast, allogeneic CAR T-cell therapies are readily available with predefined product characteristics and secured cell doses, which allows for broader applicability to a larger proportion of patients. Finally, our experience stands out as the first demonstration of activity with CAR T cells in RCC.

As previously noted, dual checkpoint inhibition (with CTLA4/PD-1 blockade) or combination treatment with ICIs and VEGF inhibitors represents the mainstay of treatment. Beyond these therapies, other targeted agents are frequently applied at the discretion of treating clinicians given the paucity of comparative efficacy data. Although prospective data are scant, some contemporary trials suggest response rates of approximately 20% in this setting (57). Therefore, although the singular CR observed with CTX130 in this study is encouraging and serves as proof-of-principle, we feel that CTX131

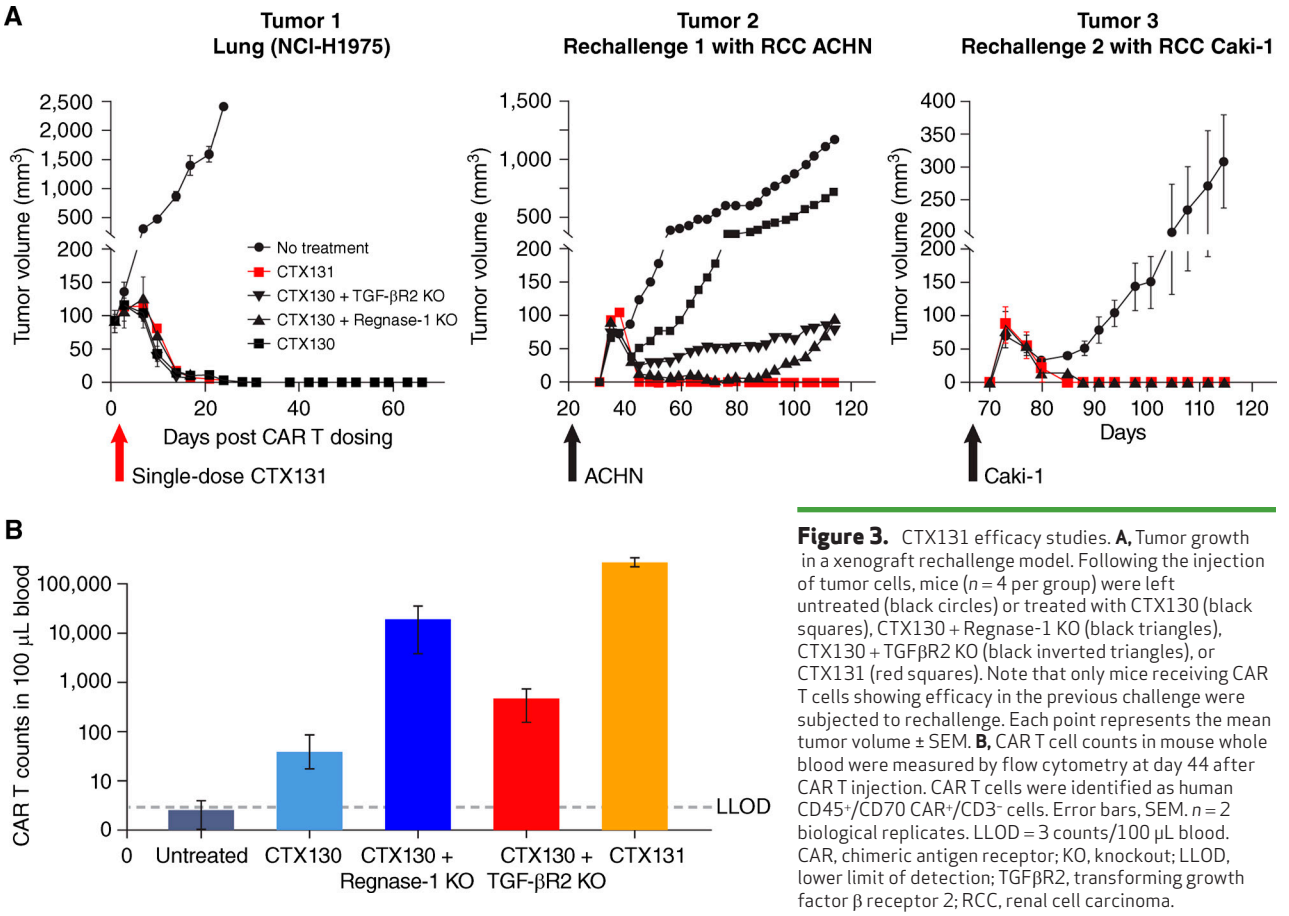

Figure 3. CTX131 efficacy studies. **A,** Tumor growth in a xenograft rechallenge model. Following the injection of tumor cells, mice ($n = 4$ per group) were left untreated (black circles) or treated with CTX130 (black squares), CTX130 + Regnase-1 KO (black triangles), CTX130 + TGFβR2 KO (black inverted triangles), or CTX131 (red squares). Note that only mice receiving CAR T cells showing efficacy in the previous challenge were subjected to rechallenge. Each point represents the mean tumor volume ± SEM. **B,** CAR T cell counts in mouse whole blood were measured by flow cytometry at day 44 after CAR T injection. CAR T cells were identified as human CD45$^+$/CD70 CAR$^+$/CD3$^-$ cells. Error bars, SEM. $n = 2$ biological replicates. LLOD = 3 counts/100 µL blood. CAR, chimeric antigen receptor; KO, knockout; LLOD, lower limit of detection; TGFβR2, transforming growth factor β receptor 2; RCC, renal cell carcinoma.

(which boasts significantly greater preclinical activity and longer persistence of CAR T cells) is better poised to generate stronger antitumor activity that could supersede current options. A phase I clinical trial is planned that will include RCC as well as other CD70-expressing tumors. Based on preliminary data from ongoing clinical trials, future trials will be focused on the next-generation CAR T product CTX131.

Limitations of the clinical data presented include the relatively small sample size, though this comes in the context of a phase I dose-escalation study. Additionally, heavily pretreated patients, who have a more substantial disease burden, were included, perhaps due to the exploratory nature of this therapy. Little is known about how this may change disease biology and responsiveness to CAR T-cell therapy. It has been established that parameters such as effector:target ratio may affect the efficacy of CAR T-cell therapies.

The findings from this study represent a proof of concept for further exploration of CD70-targeted CAR T cells in ccRCC and other CD70$^+$ malignancies and illustrate the direction of future studies evaluating the improved CD70 CAR T cell construct CTX131. Further, the Regnase-1 and TGFβR2 modifications incorporated into the CTX131 product may be applicable to other allogeneic CAR T products beyond those for ccRCC. Currently, for patients with refractory disease, treatment entails prolonged courses of VEGF inhibitors or multitargeted tyrosine kinase inhibitors, with or without ICIs. These frequently lead to chronic toxicities (e.g., diarrhea, fatigue, hand–foot syndrome), with limited durable benefits. It is our hope that the CAR T-cell approach proposed herein can offer durable responses with an acceptable safety profile and be a potential cure for these high-risk patients who otherwise have an overall poor prognosis.

METHODS

Production of CTX130 and CTX131

CTX130 was manufactured from healthy donor T cells via CRISPR-Cas9 gene editing (Supplementary Fig. S3). A recombinant adeno-associated virus (AAV) vector was used to insert an anti-CD70 CAR expression cassette into the TRAC locus, disrupting TCR expression and minimizing the risk of GvHD. Two additional guide RNAs were electroporated into cells to disrupt the expression of β2M (to minimize MHC-mediated immune rejection of the CAR T-cell product) and CD70 (to improve T-cell function and minimize fratricide).

CTX131 was manufactured from healthy donor T cells via CRISPR-Cas9 gene editing (Supplementary Fig. S4). A recombinant AAV vector was used to insert an anti-CD70 CAR expression cassette into the TRAC locus, disrupting TCR expression and minimizing the risk of GvHD. Four additional guide RNAs were electroporated into cells to disrupt expression of β2M (to minimize MHC-mediated immune rejection of the CAR T product), CD70 (to improve T-cell function), Regnase-1 (to remove the intrinsic brake on T-cell function), and TGFβR2 (to remove the extrinsic brake on T-cell antitumor activity). Editing of the TGFβR2 and Regnase-1 genes was assessed by Sanger sequencing-based tracking of indels by decomposition analysis. TGFβR2 KO was verified at the mRNA level by ddPCR. Regnase-1 protein KO was confirmed by capillary Western immunoassay using an anti-ZC3H12A rabbit polyclonal antibody (Proteintech, Rosemont, IL; catalog no. 25009-1-AP; RRID: AB_2879844).

Cell Lines

All cell lines used in the article were obtained from ATCC and were thawed and cultured according to the ATCC-recommended protocol: A498 cells (female; catalog no. HTB-44; RRID: CVCL_1056), ACHN (male; catalog no. CRL1611; RRID: CVCL_1067), Caki-1 (male; catalog no. HTB-46; RRID: CVCL_0234), NCI-H1975 (female; catalog no. CRL-5908; RRID: CVCL_1511), and MCF-7 (female; catalog no. HTB-22; RRID: CVCL_0031). Cell lines used for *in vitro* studies were not tested for *Mycoplasma* and were used for the described experiments between passages 3 and 12.

Cell lines used for *in vivo* studies were used as follows. A498 cells were authenticated on June 11, 2018; tested for *Mycoplasma* on May 23, 2018, June 1, 2018, June 6, 2018, June 13, 2018, and June 27, 2018; and used at passage P16+8. NCI-H1975 cells were authenticated on March 29, 2021, tested for *Mycoplasma* on March 31, 2021, and used at passage P8+3. ACHN cells were tested for *Mycoplasma* on May 6, 2021, and May 13, 2021 and were used at passage P5+4. No authentication of ACHN was performed prior to this study. However, the cell line was authenticated on September 22, 2022, after the completion of the study. Caki-1 cells were authenticated on March 29, 2021, tested for *Mycoplasma* on June 10, 2021, and June 17, 2021, and used at passage P17+3.

In Vitro CTX130 Studies

For the *in vitro* proliferation studies, CTX130 cells were manufactured with or without CD70 KO. After gene editing, CAR T cells were cultured for 2 weeks, and viable cells were counted at regular intervals.

For the cytotoxicity rechallenge study, CTX130 and CD70$^+$ anti-CD70 CAR T-cell cytotoxicity was assessed using a CellTiter-Glo luminescence assay. For the initial challenge, CTX130 or CD70$^+$ anti-CD70 CAR T cells were cocultured with A498 cells at a 4:1 T-cell to target-cell ratio in T-cell media with human serum and cytokines (IL2 and IL7) for 3 to 4 days. CAR T cells were then collected from the supernatant of the coculture, washed, and cocultured again with fresh A498 cells for the next challenge. The cell-killing activity of the CAR T cells was measured after a defined numbers of challenges using a CellTiter-Glo luminescence assay following a 24-hour coculture with fresh A498 cells at a 2:1 T-cell to target-cell ratio.

The cytotoxic activity of CTX130 against tumor cells expressing low (ACHN) or high (A498) levels of CD70 or with no CD70 expression (MCF7) was also assessed using a coculture system and a CellTiter-Glo luminescent cell viability assay.

In Vivo CTX130 Efficacy Studies

The ability of CTX130 to affect tumor cell growth was evaluated in a standard subcutaneous solid tumor model of CD70$^+$ RCC in NOG (NOD.Cg-Prkdc^{scid}Il2rg^{tm1Sug}/JicTac) mice. This model utilized A498 cells, which are derived from a primary RCC tumor.

In the *in vivo* study comparing the efficacy of CTX130 with CD70$^+$ anti-CD70 CAR T cells, 5 million A498 cells were injected subcutaneously into the right flank of NOG mice. When the mean tumor size reached approximately 150 mm^3, mice were either left untreated ($n = 5$) or injected i.v. with 8×10^6 CTX130 cells per mouse ($n = 5$) or with 7.5×10^6 CD70$^+$ anti-CD70 CAR T cells ($n = 4$) per mouse. Tumor volume was obtained via caliper measurements twice weekly for the duration of the study.

In the xenograft rechallenge study, 5 million A498 cells were injected subcutaneously into the right flank of NOG mice. Tumors were allowed to grow to an average size of approximately 51 mm^3, after which the tumor-bearing mice were randomized into 2 groups ($n = 5$ per group). Group 1 was left untreated, whereas groups 2 and 3 received $\approx 8 \times 10^6$ CTX130 and PD1$^-$ CTX130 cells, respectively. On day 25, a tumor rechallenge was initiated whereby 5×10^6 A498 cells were injected into the opposite (left) flank of treated mice and into a new control group. Tumor volume was obtained via caliper measurements twice weekly for the duration of the study.

GvHD was investigated in 8- to 9-week-old immunocompromised [NOD/SCID/IL2Rγnull (NSG)] mice. Animals weighed 18 to 31 grams at the start of treatment. Mice were irradiated and then administered a single dose of either unedited T cells or CTX130 (low dose, 20 million cells/mouse; high dose, 40 million cells/mouse). Mice were then monitored for symptoms of GvHD [characterized by the observation of ≥2 of the following conditions: inactivity and decreased responsiveness, respiratory distress, abnormal appearance (e.g., dull fur, hunched back, piloerection, partly closed eye, red skin, slow skin turgor, and/or skin pallor), weakness, lack of coordination, lying on side, and/or body weight loss of ≥20% over a 1-week period] throughout a 12-week period.

All animal study protocols were designed by CRISPR Therapeutics and approved by an external IACUC panel prior to study initiation.

Cytokine Secretion Analysis

The A498 adherent cancer cell line was trypsinized and seeded in ATCC-recommended media (EMEM + 10% FBS) in a 6-well plate (Corning Inc.; catalog no. 3506). Cells were cultured overnight at 37°C with 5% CO_2. On the following day, effector cells (CTX130, CTX130 + Regnase-1 KO, CTX130 + TGFβR2 KO, and CTX131) were collected from culture and seeded on the A498 cells at a 2:1 ratio in cytokine-free media (X-VIVO 15 + 5% human AB serum; Lonza, and Valley Biomedical Inc.; catalog no. HP1022). The coculture was incubated at 37°C with 5% CO_2. Cell supernatants were collected at the following time points, T0 (before incubation), T2 (2 hours after incubation), T4 (4 hours after incubation), T24 (24 hours after incubation), and T48 (48 hours after incubation), and were stored at −80°C until they were assayed for cytokine expression. Quantification of cytokine secretion was performed on the cell supernatants using the Human Magnetic Luminex Assay (R&D Systems Inc.; catalog no. LXSAHM-17) according to the manufacturer's protocol.

CTX131 Efficacy Studies

Five million NCI-H1975 cells were injected subcutaneously into the right flank of NSG (NOD.Cg-Prkdc^{scid}Il2rg^{tm1Wjl}/SzJ) mice. Tumors were allowed to grow to an average size of approximately 90 mm^3, after which the tumor-bearing mice were randomized into 5 groups ($n = 4$ per group). Group 1 was left untreated, group 2 received approximately 8 million CTX130 cells, group 3 received approximately 8 million CTX130 + Regnase-1 KO cells, group 4 received approximately 8 million CTX130 + TGFβR2 KO cells, and group 5 received approximately 8 million CTX131 cells. On day 31, a tumor rechallenge model was initiated whereby 10 million ACHN RCC cells were injected into the left flank of treated mice and into a new control group. Finally, on day 69, another rechallenge was initiated whereby 5 million Caki-1 RCC cells were injected into the right flank of treated mice and into a new control group. Rechallenges only occurred in mice receiving CAR T cells that showed efficacy in the previous challenge. Tumor volume was obtained via caliper measurements twice weekly for the duration of the study.

All animal study protocols were designed by CRISPR Therapeutics and approved by an external IACUC panel prior to study initiation.

Flow-Cytometric Analyses

Whole blood samples were collected from 2 mice in each treatment group of this study by Translational Drug Development (TD2; Scottsdale, Arizona) via submandibular survival bleed. The blood collection was performed on day 44 after CAR T-cell infusion.

Mouse whole blood samples were placed in K2-EDTA tubes at TD2 and then shipped overnight to CRISPR Therapeutics on ice packs (≈4°C). Within 24 hours of collection, 100 µL of blood was mixed with 200 µL red blood cell (RBC) lysis buffer (eBioscience 1× RBC Lysis Buffer, Thermo Fisher Scientific) in a 96-well U-bottom plate at room temperature (RT) for 10 minutes. The plate was centrifuged at 1,500 rpm for 5 minutes to collect cell pellets containing both mouse lymphocytes and human CAR T cells. To ensure complete

lysis of mouse RBCs, the cell pellets were resuspended in another 250 µL RBC lysis buffer for 10 minutes. Cell pellets were then incubated with mouse Fc receptor (FcR) block (catalog no. 101320, BioLegend; RRID: AB_1574975) at RT for 15 minutes to reduce nonspecific binding of immunoglobulin to the mouse FcRs. CAR T-cell–specific staining was achieved by incubating the cell pellets with biotinylated anti-idiotypic anti-CD70 CAR antibody (CRISPR Therapeutics, clone: 20H05-02D09-Biotin) for 30 minutes at RT. Lastly, quantification and immunophenotyping of CAR T cells were assessed with a flow-cytometric panel using the antibodies listed in Supplementary Table S2. Lymphocytes were gated on forward and side scatter areas (FSC-A and SSC-A, respectively). Single cells were then gated on FSC-A and forward scatter height (FSC-H), followed by gating for human leukocytes (human $CD45^+$/mouse $CD45^-$). CAR T cells were defined as the human $CD45^+$/anti-CD70 CAR^+/$CD3^-$ cell population.

COBALT-RCC Study Oversight

The study sponsor (CRISPR Therapeutics) designed the study protocol with oversight provided by the study steering committee and an independent data monitoring committee. The research protocol was approved by the CRISPR Therapeutics review board/ethics committee, and participants provided written informed consent. The study was performed in accordance with the principles set forth in the Declaration of Helsinki. All authors had access to the data and approved the decision to submit the manuscript for publication. All the authors vouch for the accuracy and completeness of the data presented here, and the representatives of CRISPR Therapeutics vouch for the fidelity of the trial to the protocol.

COBALT-RCC Trial Design and Eligibility

COBALT-RCC (NCT04438083) is an open-label, multicenter, phase I study evaluating the safety, efficacy, and pharmacokinetics of CTX130 in patients with unresectable or metastatic, relapsed, or refractory ccRCC. Eligibility was limited to patients ages ≥18 years who had prior exposure to an ICI and a VEGF inhibitor.

Patients received standard lymphodepletion with fludarabine/ cyclophosphamide (30 mg/m^2 fludarabine and 500 mg/m^2 cyclophosphamide i.v. daily for 3 days) followed by a single infusion of CTX130 (DL1, 3×10^7 CAR T cells; DL2, 1×10^8 CAR T cells; DL3, 3×10^8 CAR T cells; DL4, 9×10^8 CAR T cells; Supplementary Fig. S5; Supplementary Fig. S6). A standard 3+3 trial design was used, in which 3 to 6 subjects were enrolled at each dose level depending on the occurrence of DLTs.

The dosing of CTX130 was informed by prior clinical experience with CAR T cell therapies. For example, the starting dose of CTX130 (3×10^7 CAR T cells) is at least 0.32 log lower than the approved doses of autologous CD19-directed CAR T cells for non-Hodgkin lymphoma and more than 1 log lower than the average starting dose used in many published clinical trials with autologous CAR T-cell therapies directed at solid tumors (58, 59).

The primary objective of this study was to assess the safety of CTX130 by the incidence of AEs, defined as DLTs. A secondary objective was to assess the efficacy of CTX130, as measured by ORR according to RECIST guidelines (v1.1). The response assessment was performed locally by the investigator in this dose-escalation phase. Other secondary objectives were to assess PFS, OS, time to response, and duration of response and to characterize pharmacokinetics (expansion and persistence) of CTX130 in the blood.

Patients were permitted to receive ≤2 additional doses of CTX130 after lymphodepleting chemotherapy based on the investigator's decision and in consultation with the sponsor's medical monitor. To be considered for redosing, patients must have either: (i) achieved a PR or CR after the initial or second CTX130 infusion and have an increase in tumor size (sum of target lesion diameters) of ≥10% within 2 years of the last dose or (ii) achieved SD or progressive disease with significant clinical benefit at the day 42 study visit after the most recent CTX130 infusion. Repeat dosing decisions were based on local computed tomography scan/assessment. The earliest time at which a patient could be redosed was 8 weeks after the initial or second CTX130 infusion.

Following CTX130 infusion, patients were monitored for acute toxicities (days 1–28), including CRS, ICANS, GvHD, and other AEs. After the 28-day acute toxicity monitoring period, patients will be monitored for ≤5 years and assessed for ccRCC response (with initial efficacy assessment at day 42), disease progression, and survival. Monitoring during this period will include physical exams, laboratory and imaging assessments, and AE assessments.

COBALT-RCC Patient Samples

Whole blood and tumor samples were collected from patients in the COBALT-RCC trial according to the collection regimen outlined in the trial protocol. Where posttreatment tumor samples were collected, they were collected from the same organ site as the screening sample. All patients provided written consent.

ddPCR

DNA was extracted from whole blood samples using the Qiagen Blood DNA Midi Kit (catalog no. 816-0551, Qiagen). DNA samples were digested with the BamHI (catalog no. 852-0449, New England Biolabs) and KpnI (catalog no. 852-0450, New England Biolabs) enzymes. The ddPCR reaction was prepared with 2× ddPCR Supermix (Bio-Rad), FAM dye/MGB probe targeting the CAR insert (Thermo Fisher), VIC dye/QSY probe targeting the reference gene ABHD4 (Thermo Fisher), deoxynucleoside triphosphates, and $MgCl_2$. Droplets were generated automatically with the QX200 Droplet Generator (Bio-Rad; RRID: SCR_019707). The reactions were placed in the thermal cycler and subjected to the following conditions: enzyme activation at 95°C for 10 minutes; 45 cycles of 94°C for 30 seconds, 64°C for 1 minute, and 72°C for 2 minutes; 98°C for 10 minutes; and a final 4°C step for 2 hours. Droplet acquisition and analysis were performed with the QX200 Droplet Reader and QuantaSoft Software (Bio-Rad). The number of copies of the CAR construct (per microgram) was plotted against the visit days, and the peak number of copies of the CAR construct (per microgram) was plotted against the DL using GraphPad Prism by Dotmatics.

CD70 IHC

IHC analysis of CD70 was performed using automated detection at RT on the Leica BOND RX autostainer (Leica Biosystems). Specimens were sectioned at 5-µm thickness, mounted onto positively charged glass slides, dried, and baked for 30 minutes at 60°C. Tissue slides were deparaffinized and rehydrated with xylene (catalog no. 134B, Medical Chemical Corporation) followed by a graded ethanol series (100% to 80%, catalog no. 374B, Medical Chemical Corporation). Tissue slides were rinsed in distilled water prior to being placed in the Leica BOND RX autostainer. Heat-induced epitope retrieval was performed with BOND ER2 for 20 minutes at 100°C. Tissue slides were incubated in Peroxide Block (catalog no. DS9800, BOND Polymer Refine Detection Kit, Leica) for 5 minutes, ISH/IHC SuperBlock (catalog no. PV6122, Leica) for 10 minutes, and CD70 primary antibody (10 µg/mL Clone 4E6G9, CRISPR Therapeutics) or isotype control for 30 minutes. For detection, tissue slides were incubated in Post Primary (BOND Polymer Refine Detection Kit, Leica) for 8 minutes, Polymer (BOND Polymer Refine Detection Kit, Leica) for 8 minutes, and Mixed DAB Refine for 10 minutes. Slides were counterstained with hematoxylin (BOND Polymer Refine Detection Kit, Leica) for 5 minutes. The tissue slides were removed from the autostainer, dehydrated, and cleared with a graded ethanol series and xylene. Coverslip mounting was performed using an automated tape coverslipper (Sakura Fine-Tek). Staining was evaluated by a pathologist under a light microscope. Percent CD70 positivity was plotted for each visit day using GraphPad Prism by Dotmatics.

Data Availability

The deidentified data that underlie the results reported in the article, as well as information from the protocol, will be available following article publication. Researchers should submit a methodologically sound proposal for materials or data to medicalaffairs@crisprtx.com.

Authors' Disclosures

S.K. Pal reports other support from CRISPR, Ipsen, and Exelixis during the conduct of the study. B. Tran reports other support from CRISPR during the conduct of the study; grants and personal fees from Amgen, Astra Zeneca, Astellas, BMS, MSD, Merck, Pfizer, Janssen, Bayer, Ipsen, and Sanofi and grants from Roche outside the submitted work. J.B. Haanen reports grants from Amgen, Asher Bio, BMS, BioNTech, and Sastra Cell Therapy outside the submitted work; and provided advice to Agenus, AZ, BMS, CureVac, GSK, Imcyse, Iovance Bio, Immunocore, Ipsen, Merck Serono, MSD, Molecular Partners, Obsedian Tx, Novartis, Orgenesis, Pfizer, Roche/Genentech, Sanofi, and Third Rock Ventures and participated in the SAB of Achilles Tx, BioNTech, Instil Bio, Neogene Therapeutics (AZ), PokeAcell, Sastra Cell Therapy, Scenic, and T-Knife. M.E. Hurwitz reports other support from CRISPR Therapeutics during the conduct of the study; other support from Affini-T therapeutics, Exelixis, Pliant Therapeutics, Janssen, Regeneron, TScan, and grants from Astra Zeneca and Iovance outside the submitted work. A. Sacher reports other support from CRISPR Therapeutics during the conduct of the study; other support from Amgen, AstraZeneca, BMS, CRISPR Therapeutics, Lilly/LOXO, Genentech, GSK, Iovance, Merck, Pfizer, Spectrum, and Merck outside the submitted work. L.E. Budde reports other support from City of Hope during the conduct of the study; personal fees from BMS, Kite Pharma, and Janssen outside the submitted work; in addition, L.E. Budde has a patent for CD33CAR issued. S.J. Harrison reports other support from AbbVie, Amgen, Celgene/ BMB, CSL Bering, GSK, grants, nonfinancial and other support from Janssen Cilag, Novartis, Kite/Gilead, other support from Roche/ Genetec, Haemalogix, and Eusa outside the submitted work. S. Klobuch reports Advisory Board for Regeneron Pharmaceuticals. S.S. Patel reports personal fees from Sanofi outside the submitted work. L. Meza reports personal fees from Ipsen outside the submitted work. M. Dequeant reports a patent for genetically engineered T cells with Regnase-1 and TGFBRII disruption have improved functionality and persistence issued, a patent for Anti-idiotype antibodies targeting anti-CD70 chimeric antigen receptor issued, a patent for Methods and compositions for treating cancer issued, a patent for CD70$^+$ solid tumor therapy using genetically engineered T cells targeting CD70 pending, a patent for methods for manufacturing genetically engineered CAR T cells pending, and a patent for Renal Cell Carcinoma Therapy using genetically engineered T cells targeting CD70 pending. A. Ma reports other support from CRISPR Therapeutics outside the submitted work. Q.A. He reports being an employee of CRISPR Therapeutics. H. Dar reports other support from CRISPR Therapeutics during the conduct of the study. P.K. Morrow reports other support from CRISPR Therapeutics during the conduct of the study. N. Agarwal reports grants from CRISPR during the conduct of the study; personal fees from Lilly, Gilead and Foundation Medicine outside the submitted work; and Neeraj N. Agarwal has received honorarium before May 2021 and during his lifetime for consulting to Astellas, AstraZeneca, Aveo, Bayer, Bristol Myers Squibb, Calithera, Clovis, Eisai, Eli Lilly, EMD Serono, Exelixis, Foundation Medicine, Genentech, Gilead, Janssen, Merck, MEI Pharma, Nektar, Novartis, Pfizer, Pharmacyclics, and Seattle Genetics; and has received research funding during his lifetime from Arnivas, Astellas, AstraZeneca, Bavarian Nordic, Bayer, Bristol Meyers Squibb, Calithera, Celldex, Clovis, CRISPR Therapeutics, Eisai, Eli Lilly, EMD Serono, Exelixis, Genentech, Gilead, Glaxo Smith Kline, Immunomedics, Janssen, Lava, Medivation, Merck, Nektar, Neoleukin, New Link Genetics, Novartis, Oric, Pfizer, Prometheus, Rexahn, Roche, Sanofi, Seattle Genetics, Takeda, and Tracon. No disclosures were reported by the other authors.

Authors' Contributions

S.K. Pal: Conceptualization, data curation, formal analysis, supervision, validation, investigation, methodology, writing–original draft, project administration, writing–review and editing. **B. Tran:** Resources, methodology, writing–review and editing. **J.B. Haanen:** Investigation, writing–review and editing. **M.E. Hurwitz:** Conceptualization, investigation, methodology, writing–review and editing. **A. Sacher:** Formal analysis, supervision, investigation, methodology, project administration, writing–review and editing. **N.M. Tannir:** Resources, writing–review and editing. **L.E. Budde:** Data curation, investigation, writing–review and editing. **S.J. Harrison:** Resources, supervision, project administration, writing–review and editing. **S. Klobuch:** Investigation, writing–review and editing. **S.S. Patel:** Writing–review and editing. **L. Meza:** Resources, data curation, investigation, writing–review and editing. **M. Dequeant:** Conceptualization, formal analysis, supervision, validation, visualization, methodology, writing–original draft, writing–review and editing. **A. Ma:** Data curation, formal analysis, visualization, methodology, writing–original draft, project administration, writing–review and editing. **Q.A. He:** Data curation, formal analysis, methodology, writing–review and editing. **L.M. Williams:** Conceptualization, data curation, formal analysis, validation, visualization, writing–original draft, writing–review and editing. **A. Keegan:** Data curation, formal analysis, writing–review and editing. **E.B. Gurary:** Data curation, formal analysis, writing–original draft. **H. Dar:** Conceptualization, visualization, writing–review and editing. **S. Karnik:** Conceptualization, data curation, formal analysis, investigation, methodology, writing–review and editing. **C. Guo:** Data curation, formal analysis, investigation, visualization, methodology, writing–review and editing. **H. Heath:** Data curation, formal analysis, investigation, visualization, methodology, writing–review and editing. **R.R. Yuen:** Data curation, formal analysis, investigation, visualization, methodology, writing–review and editing. **P.K. Morrow:** Conceptualization, resources, data curation, formal analysis, supervision, funding acquisition, investigation, methodology, project administration, writing–review and editing. **N. Agarwal:** Resources, data curation, formal analysis, supervision, investigation, methodology, writing–original draft, project administration, writing–review and editing. **S.A. Srour:** Supervision, validation, investigation, project administration, writing–review and editing.

Acknowledgments

The authors would like to thank Adele Musicant, PhD, of PRECISIONscientia in Yardley, Pennsylvania, for medical writing assistance. This study was assisted, sponsored, and funded by CRISPR Therapeutics.

Note

Supplementary data for this article are available at Cancer Discovery Online (http://cancerdiscovery.aacrjournals.org/).

Received January 19, 2024; revised March 8, 2024; accepted March 22, 2024; published first April 4, 2024.

REFERENCES

1. Junker K, Hindermann W, von Eggeling F, Diegmann J, Haessler K, Schubert J. CD70: a new tumor specific biomarker for renal cell carcinoma. J Urol 2005;173:2150–3.
2. Siegel RL, Miller KD, Wagle NS, Jemal A. Cancer statistics, 2023. CA Cancer J Clin 2023;73:17–48.
3. Hsieh JJ, Purdue MP, Signoretti S, Swanton C, Albiges L, Schmidinger M, et al. Renal cell carcinoma. Nat Rev Dis Primers 2017;3:17009.

4. Buchbinder EI, Dutcher JP, Daniels GA, Curti BD, Patel SP, Holtan SG, et al. Therapy with high-dose interleukin-2 (HD IL-2) in metastatic melanoma and renal cell carcinoma following PD1 or PDL1 inhibition. J Immunother Cancer 2019;7:49.
5. Clark JI, Wong MKK, Kaufman HL, Daniels GA, Morse MA, McDermott DF, et al. Impact of sequencing targeted therapies with high-dose interleukin-2 immunotherapy: an analysis of outcome and survival of patients with metastatic renal cell carcinoma from an on-going observational IL-2 clinical trial: PROCLAIM(SM). Clin Genitourin Cancer 2017;15:31–41.
6. Negrier S, Escudier B, Lasset C, Douillard JY, Savary J, Chevreau C, et al. Recombinant human interleukin-2, recombinant human interferon alfa-2a, or both in metastatic renal-cell carcinoma. N Engl J Med 1998;338:1272–8.
7. Motzer RJ, Jonasch E, Agarwal N, Alva A, Baine M, Beckermann K, et al. Kidney cancer, version 3.2022, NCCN clinical practice guidelines in oncology. J Natl Compr Canc Netw 2022;20:71–90.
8. Rini BI, Plimack ER, Stus V, Gafanov R, Hawkins R, Nosov D, et al. Pembrolizumab plus axitinib versus sunitinib for advanced renal-cell carcinoma. N Engl J Med 2019;380:1116–27.
9. Motzer RJ, Tannir NM, McDermott DF, Aren Frontera O, Melichar B, Choueiri TK, et al. Nivolumab plus ipilimumab versus sunitinib in advanced renal-cell carcinoma. N Engl J Med 2018;378:1277–90.
10. Motzer R, Alekseev B, Rha SY, Porta C, Eto M, Powles T, et al. Lenvatinib plus pembrolizumab or everolimus for advanced renal cell carcinoma. N Engl J Med 2021;384:1289–300.
11. Choueiri TK, Powles T, Burotto M, Escudier B, Bourlon MT, Zurawski B, et al. Nivolumab plus cabozantinib versus sunitinib for advanced renal-cell carcinoma. N Engl J Med 2021;384:829–41.
12. Auvray M, Auclin E, Barthelemy P, Bono P, Kellokumpu-Lehtinen P, Gross-Goupil M, et al. Second-line targeted therapies after nivolumab-ipilimumab failure in metastatic renal cell carcinoma. Eur J Cancer 2019;108:33–40.
13. Barata PC, De Liano AG, Mendiratta P, Crolley V, Szabados B, Morrison L, et al. The efficacy of VEGFR TKI therapy after progression on immune combination therapy in metastatic renal cell carcinoma. Br J Cancer 2018;119:160–3.
14. Nadal R, Amin A, Geynisman DM, Voss MH, Weinstock M, Doyle J, et al. Safety and clinical activity of vascular endothelial growth factor receptor (VEGFR)-tyrosine kinase inhibitors after programmed cell death 1 inhibitor treatment in patients with metastatic clear cell renal cell carcinoma. Ann Oncol 2016;27:1304–11.
15. Claus C, Riether C, Schurch C, Matter MS, Hilmenyuk T, Ochsenbein AF. CD27 signaling increases the frequency of regulatory T cells and promotes tumor growth. Cancer Res 2012;72:3664–76.
16. Flieswasser T, Camara-Clayette V, Danu A, Bosq J, Ribrag V, Zabrocki P, et al. Screening a broad range of solid and haematological tumour types for CD70 expression using a uniform IHC methodology as potential patient stratification method. Cancers 2019;11:1161.
17. Jilaveanu LB, Sznol J, Aziz SA, Duchen D, Kluger HM, Camp RL. CD70 expression patterns in renal cell carcinoma. Hum Pathol 2012;43:1394–9.
18. Lens SM, Baars PA, Hooibrink B, van Oers MH, van Lier RA. Antigen-presenting cell-derived signals determine expression levels of CD70 on primed T cells. Immunology 1997;90:38–45.
19. O'Neill RE, Du W, Mohammadpour H, Alqassim E, Qiu J, Chen G, et al. T cell-derived CD70 delivers an immune checkpoint function in inflammatory T cell responses. J Immunol 2017;199:3700–10.
20. Diegmann J, Junker K, Loncarevic IF, Michel S, Schimmel B, von Eggeling F. Immune escape for renal cell carcinoma: CD70 mediates apoptosis in lymphocytes. Neoplasia 2006;8:933–8.
21. Aftimos P, Rolfo C, Rottey S, Offner F, Bron D, Maerevoet M, et al. Phase I dose-escalation study of the anti-CD70 antibody ARGX-110 in advanced malignancies. Clin Cancer Res 2017;23:6411–20.
22. Pal SK, Forero-Torres A, Thompson JA, Morris JC, Chhabra S, Hoimes CJ, et al. A phase 1 trial of SGN-CD70A in patients with CD70-positive, metastatic renal cell carcinoma. Cancer 2019;125:1124–32.
23. Buchan SL, Rogel A, Al-Shamkhani A. The immunobiology of CD27 and OX40 and their potential as targets for cancer immunotherapy. Blood 2018;131:39–48.
24. Ruf M, Mittmann C, Nowicka AM, Hartmann A, Hermanns T, Poyet C, et al. pVHL/HIF-regulated CD70 expression is associated with infiltration of $CD27^+$ lymphocytes and increased serum levels of soluble CD27 in clear cell renal cell carcinoma. Clin Cancer Res 2015;21:889–98.
25. Wang QJ, Hanada K, Robbins PF, Li YF, Yang JC. Distinctive features of the differentiated phenotype and infiltration of tumor-reactive lymphocytes in clear cell renal cell carcinoma. Cancer Res 2012;72:6119–29.
26. Massard C, Soria JC, Krauss J, Gordon M, Lockhart AC, Rasmussen E, et al. First-in-human study to assess safety, tolerability, pharmacokinetics, and pharmacodynamics of the anti-CD27L antibody-drug conjugate AMG 172 in patients with relapsed/refractory renal cell carcinoma. Cancer Chemother Pharmacol 2019;83:1057–63.
27. Tannir NM, Forero-Torres A, Ramchandren R, Pal SK, Ansell SM, Infante JR, et al. Phase I dose-escalation study of SGN-75 in patients with CD70-positive relapsed/refractory non-Hodgkin lymphoma or metastatic renal cell carcinoma. Invest New Drugs 2014;32:1246–57.
28. Owonikoko TK, Hussain A, Stadler WM, Smith DC, Kluger H, Molina AM, et al. First-in-human multicenter phase I study of BMS-936561 (MDX-1203), an antibody-drug conjugate targeting CD70. Cancer Chemother Pharmacol 2016;77:155–62.
29. Lin H, Cheng J, Mu W, Zhou J, Zhu L. Advances in Universal CAR-T cell therapy. Front Immunol 2021;12:744823.
30. Hu W, Zi Z, Jin Y, Li G, Shao K, Cai Q, et al. CRISPR/Cas9-mediated PD-1 disruption enhances human mesothelin-targeted CAR T cell effector functions. Cancer Immunol Immunother 2019;68:365–77.
31. Rupp LJ, Schumann K, Roybal KT, Gate RE, Ye CJ, Lim WA, et al. CRISPR/Cas9-mediated PD-1 disruption enhances anti-tumor efficacy of human chimeric antigen receptor T cells. Sci Rep 2017;7:737.
32. Guo X, Jiang H, Shi B, Zhou M, Zhang H, Shi Z, et al. Disruption of PD-1 enhanced the anti-tumor activity of chimeric antigen receptor T cells against hepatocellular carcinoma. Front Pharmacol 2018;9:1118.
33. Dequeant M, Sagert J, Kalaitzidis D, Yu H, Porras A, McEwan B, et al. CD70 knockout: a novel approach to augment CAR-T cell function. Cancer Res 81, 2021 (suppl 13; abstr 1537).
34. Ko JJ, Xie W, Kroeger N, Lee JL, Rini BI, Knox JJ, et al. The International Metastatic Renal Cell Carcinoma Database Consortium model as a prognostic tool in patients with metastatic renal cell carcinoma previously treated with first-line targeted therapy: a population-based study. Lancet Oncol 2015;16:293–300.
35. Lee DW, Santomasso BD, Locke FL, Ghobadi A, Turtle CJ, Brudno JN, et al. ASTCT consensus grading for cytokine release syndrome and neurologic toxicity associated with immune effector cells. Biol Blood Marrow Transplant 2019;25:625–38.
36. Neelapu SS, Locke FL, Bartlett NL, Lekakis LJ, Miklos DB, Jacobson CA, et al. Axicabtagene ciloleucel CAR T-cell therapy in refractory large B-cell lymphoma. N Engl J Med 2017;377:2531–44.
37. Abramson JS, Palomba ML, Gordon LI, Lunning MA, Wang M, Arnason J, et al. Lisocabtagene maraleucel for patients with relapsed or refractory large B-cell lymphomas (TRANSCEND NHL 001): a multicentre seamless design study. Lancet 2020;396:839–52.
38. Iyer SP, Sica RA, Ho PJ, Hu B, Zain J, Prica A, et al. S262 The COBALT-LYM study of CTX130: a phase 1 dose escalation study of CD70-targeted allogeneic CRISPR-Cas9–engineered CAR T cells in patients with relapsed/refractory (R/R) T-cell malignancies. Hemasphere 2022;6:163–4.
39. Wrocklage C, Lin S, le Mercier I, Bullock C, Cadzow L, Hohmann A, et al. KSQ-004: Unbiased pair-wise discovery of SOCS1 and Regnase-1 as the top CRISPR/Cas9 dual-edit combination enhancing *in vivo* TIL potency against solid tumors. Poster presented at: Society for Immunotherapy of Cancer Annual Meeting; November 10–14, 2021: Washington, DC.
40. Terrett JA, Kalaitzidis D, Dequeant M-L, Karnik S, Ghonime M, Guo C, et al. CTX112 and CTX131: next-generation CRISPR/Cas9-engineered allogeneic (allo) CAR T cells incorporating novel edits that increase potency and efficacy in the treatment of lymphoid and solid tumors. Cancer Res 83, 2023 (suppl 7; abstr ND02).
41. Matsushita K, Takeuchi O, Standley DM, Kumagai Y, Kawagoe T, Miyake T, et al. Zc3h12a is an RNase essential for controlling immune responses by regulating mRNA decay. Nature 2009;458:1185–90.
42. Uehata T, Iwasaki H, Vandenbon A, Matsushita K, Hernandez-Cuellar E, Kuniyoshi K, et al. Malt1-induced cleavage of Regnase-1 in CD4(+) helper T cells regulates immune activation. Cell 2013;153:1036–49.

43. Kidoya H, Muramatsu F, Shimamura T, Jia W, Satoh T, Hayashi Y, et al. Regnase-1-mediated post-transcriptional regulation is essential for hematopoietic stem and progenitor cell homeostasis. Nat Commun 2019;10:1072.
44. Wei J, Long L, Zheng W, Dhungana Y, Lim SA, Guy C, et al. Targeting REGNASE-1 programs long-lived effector T cells for cancer therapy. Nature 2019;576:471–6.
45. Jeltsch KM, Heissmeyer V. Regulation of T cell signaling and autoimmunity by RNA-binding proteins. Curr Opin Immunol 2016;39:127–35.
46. Sanjabi S, Oh SA, Li MO. Regulation of the immune response by TGF-beta: from conception to autoimmunity and infection. Cold Spring Harb Perspect Biol 2017;9:a022236.
47. Tang N, Cheng C, Zhang X, Qiao M, Li N, Mu W, et al. TGF-beta inhibition via CRISPR promotes the long-term efficacy of CAR T cells against solid tumors. JCI Insight 2020;5:e133977.
48. Thomas DA, Massague J. TGF-beta directly targets cytotoxic T cell functions during tumor evasion of immune surveillance. Cancer Cell 2005;8:369–80.
49. Batlle E, Massague J. Transforming growth factor-beta signaling in immunity and cancer. Immunity 2019;50:924–40.
50. Srour SA, Akin S. Chimeric antigen receptor T-cell therapy for solid tumors: the past and the future. J Immunother Precis Oncol 2023;6:19–30.
51. Qi C, Gong J, Li J, Liu D, Qin Y, Ge S, et al. Claudin18.2-specific CAR T cells in gastrointestinal cancers: phase 1 trial interim results. Nat Med 2022;28:1189–98.
52. Brown CE, Alizadeh D, Starr R, Weng L, Wagner JR, Naranjo A, et al. Regression of glioblastoma after chimeric antigen receptor T-cell therapy. N Engl J Med 2016;375:2561–9.
53. Louis CU, Savoldo B, Dotti G, Pule M, Yvon E, Myers GD, et al. Antitumor activity and long-term fate of chimeric antigen receptor-positive T cells in patients with neuroblastoma. Blood 2011;118:6050–6.
54. Narayan V, Barber-Rotenberg JS, Jung IY, Lacey SF, Rech AJ, Davis MM, et al. PSMA-targeting TGFbeta-insensitive armored CAR T cells in metastatic castration-resistant prostate cancer: a phase 1 trial. Nat Med 2022;28:724–34.
55. Dorff TB, Blanchard S, Martirosyan H, Adkins L, Dhapola G, Moriarty A, et al. Phase 1 study of PSCA-targeted chimeric antigen receptor (CAR) T cell therapy for metastatic castration-resistant prostate cancer (mCRPC). J Clin Oncol 40, 2022;(suppl. 6; abstr 91).
56. Lamers CH, Sleijfer S, van Steenbergen S, van Elzakker P, van Krimpen B, Groot C, et al. Treatment of metastatic renal cell carcinoma with CAIX CAR-engineered T cells: clinical evaluation and management of on-target toxicity. Mol Ther 2013;21:904–12.
57. Rini BI, Pal SK, Escudier BJ, Atkins MB, Hutson TE, Porta C, et al. Tivozanib versus sorafenib in patients with advanced renal cell carcinoma (TIVO-3): a phase 3, multicentre, randomised, controlled, open-label study. Lancet Oncol 2020;21:95–104.
58. Guo Y, Feng K, Liu Y, Wu Z, Dai H, Yang Q, et al. Phase I study of chimeric antigen receptor-modified T cells in patients with EGFR-positive advanced biliary tract cancers. Clin Cancer Res 2018;24:1277–86.
59. Kershaw MH, Westwood JA, Parker LL, Wang G, Eshhar Z, Mavroukakis SA, et al. A phase I study on adoptive immunotherapy using gene-modified T cells for ovarian cancer. Clin Cancer Res 2006;12:6106–15.